CrossMark

# A novel dual-band dual-polarized shared-aperture antenna with high isolation

Jiachen Xu [iD], Bozhang Lan, Jiakai Zhang, Chenjiang Guo and Jun Ding

School of Electronics and Information, Northwestern Polytechnic University, Xi'an 710129, China

## Abstract

This paper presents a novel dual-band (DB) dual-polarized (DP) shared aperture antenna with high isolation by using a combination of microstrip dipoles and dielectric resonator antennas (DRAs) for S and C bands, respectively. In the S band, two sets of proximity coupled stacked microstrip dipoles which crossed at the center are employed to achieve dual-linear polarization (DLP) and obtain desired bandwidth (BW), isolation, and pure polarization. The rectangle DRA with hybrid feed is selected as the C band element for its advantages of small base area and high isolation, and a $2 \times 2$ array is presented with the "pair-wise" anti-phase feed technique to achieve a low cross-polarized level. Moreover, benefited from the back feed scheme, the proposed antenna has a symmetrical structure and has the potential of expanding into a larger aperture. The proposed antenna has been manufactured and measured, and the results agree well with simulations, which prove the validity of the proposed design.

## Introduction

Nowadays, there has been a growing demand for modern wireless applications such as satellite communication, earth-observing, modern radar, etc. Antennas featuring dual-band and dual-polarized (DBDP) have received increasing attention [1, 2]. In a wireless communication system, dual-band operations could improve the versatility of the systems, and dual-polarized technique could be used for increasing the communication capacity and combating anti-multipath-fading [3]. In a radar system, DBDP operations can provide finer resolution and obtain better penetration or reflection data from various scatterers [4]. Furthermore, antennas are always hoped to have a compact size and lightweight, so shared-aperture technology has attracted people's attention. By sharing the same aperture, antennas working at different bands can reduce the volume and mass, and the aperture efficiency could be increased with little effect on performance.

Therefore, shared-aperture antennas have been studied, and several approaches are proposed. The perforated structure has been widely used, and antennas of both bands share a common aperture by etching perforations on lower band antennas. In this structure, the frequency ratio (FR) of two bands can be adjusted by the number of perforations on lower band antenna, and some common solutions are one perforation [3, 5], four perforations [4, 6, 7], and 16 perforations [8–10]. The perforated structure is attractive benefited from higher aperture efficiency, because, besides the spacing of the lower frequency elements, perforations on lower frequency patches can also be used by higher frequency antennas. However, the size of perforations is a critical issue to tackle in that big perforations affect the performance of lower frequency patches, and small perforations cause strong mutual coupling. Comparatively, the configurations of interlaced low-frequency elements with high-frequency patches are more flexible, because the low frequency interlaced elements could be dipoles [11–13], square ring antennas [14], cross dielectric resonator antennas (DRAs) [15], corner-etched circular patches [16], and patches[1, 17, 18], and any FR can be realized theoretically [13]. Beyond that, some derivative models are also proposed [19, 20]. Stacked structure is employed in [21, 22]. In [21], Ku-band array is on the upper layer, and P-band patch is on the lower layer used as an antenna and ground of Ku band. In [22], the S-band antenna uses the stacked patches, where the upper parasitic patch is used to enhance gain and bandwidth as well as ground for the X-band excited patch. In a stacked structure shared-aperture antenna, the antenna of the lower band does not need to be miniaturized and perforated, so the low Q factor is easier to obtain and featuring wide bandwidth. However, limited by this structure, it is challenging to form arrays for both bands flexibly.

For both configurations, using the ground to separate the feed networks of two bands is a practical method for band isolation enhancing, but there is still room for improvement. To date, most of the reported work use printed antennas for two bands, the printed antennas in a narrow area would inevitably produce severe parasitic capacitances which have a terrible influence on band isolation. Moreover, the mutual interference between bands brings many
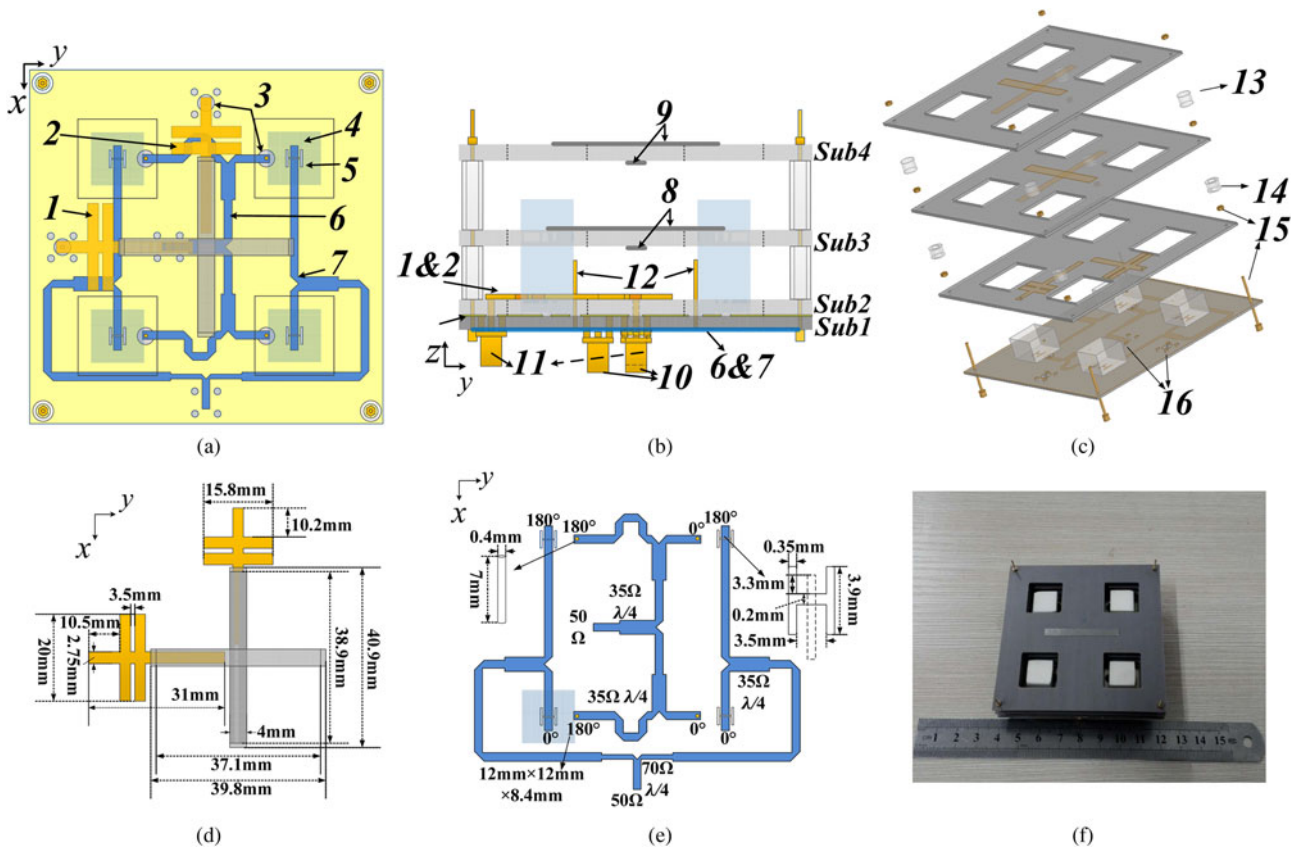
**Fig. 1.** Structure of proposed DBDP shared-aperture antenna. (a) Top view. (b) Side view. (c) Exploded view. (d) S band antennas and feed lines. (e) C band array and feed network. (f) Photo of proposed antenna.

troubles for designing, manufacturing, and assembling the shared aperture antennas, it is may not be an issue in a large FR (FR ≥ 4) shared aperture antenna but very significant for small FR (FR < 4) antennas.

This paper presents a novel small FR (about 1:2) S/C DBDP shared-aperture antenna with a combination of interlaced stacked printed dipoles and rectangle DRAs. Coupling between bands and mutual interference is very low by the use of DRAs because the DRA has non-metal character and it wouldn't produce any parasitic capacitance with nearby metal. Besides, DRA also has several advantages such as small size, ease of excitation, small mutual coupling, low loss, and high radiation efficiency [14, 23], so DRA is very suitable for shared aperture antenna applications. The proposed antenna has good bandwidth and radiation characteristics in both bands, and the interference between bands is also researched.

## Antenna design

The proposed antenna is working in the S band (2.7–3 GHz) and C band (5.3–5.7 GHz), and the FR is about 1:2, so the element spacing is 2:1. Considering the relationship between the gain and element spacing [24], the length of the proposed antenna (which is the same as the spacing of S band element if larger array is expanded), is 80 mm (0.76λ at 2.85 GHz), so the spacing of C band element is 40 mm (0.73λ at 5.5 GHz). The configuration of the DBDP shared-aperture antenna is shown in Fig. 1, and detailed information is shown in Table 1. The prototype antenna consists of

four layers, and the parameters of substrates are shown in Table 2. The four substrates are fixed by screws and nuts (considered in the simulation model), and hard plastic tubes are used to support the necessary spacing between Sub2 and Sub3, Sub3 and Sub5 respectively. The Sub-Miniature-A (SMA) connectors for horizontal (H) and vertical (V) polarization of both bands are soldered at the bottom to make the sides of the antenna flat for the potential demand of multi-antenna piecing and aperture expanding. Remarkably, the flange of C band SMA connectors should keep a small gap with the Sub1 and feed lines to prevent short circuit. Furthermore, the height of the whole antenna is determined by the multilayer structure of S band, so the uses of DRAs won't add any additional height for the proposed antenna.

Proximity coupled, stacked microstrip dipole is selected as the radiating element for S band, and the use of dipoles instead of slots can avoid the backward radiation and bring more convenience for broadening the bandwidth. The dimension of the printed dipoles can be approximately calculated, where $l_{dipole}$ is the length of the printed dipole, $c$ is the speed of light in free space, $\varepsilon_{eff}$ is the effective dielectric constant, and $f_0$ is the center frequency of the S-band operation, which is 2.85 GHz in this design:

$$l_{dipole} \approx \frac{c}{2f_0\sqrt{\varepsilon_{eff}}} \qquad (1)$$

F4BM220 ($\varepsilon_r = 2.2$) is selected as the substrate of S band for broadening the bandwidth. Double tuning stubs are used in feed lines to provide more freedom for impedance matching

**Table 1.** Comments for the structure of DBDP shared-aperture antenna subarray

| Number | Comments | Number | Comments |
|--------|----------|--------|----------|
| 1 | S band feed line (VP) | 9 | S band parasitic diploe |
| 2 | S band feed line (HP) | 10 | C band SMA |
| 3 | Circular holes on ground | 11 | S band SMA |
| 4 | DRA | 12 | Fed-probe |
| 5 | "H" slots on ground | 13 | 4 mm-long-hard plastic tube |
| 6 | C band feeding network (VP) | 14 | 3.5 mm-long-hard plastic tube |
| 7 | C band feeding network (HP) | 15 | Nuts and screws |
| 8 | S band driven diploe | 16 | Through-holes for SMA |

**Table 2.** Details of substrates

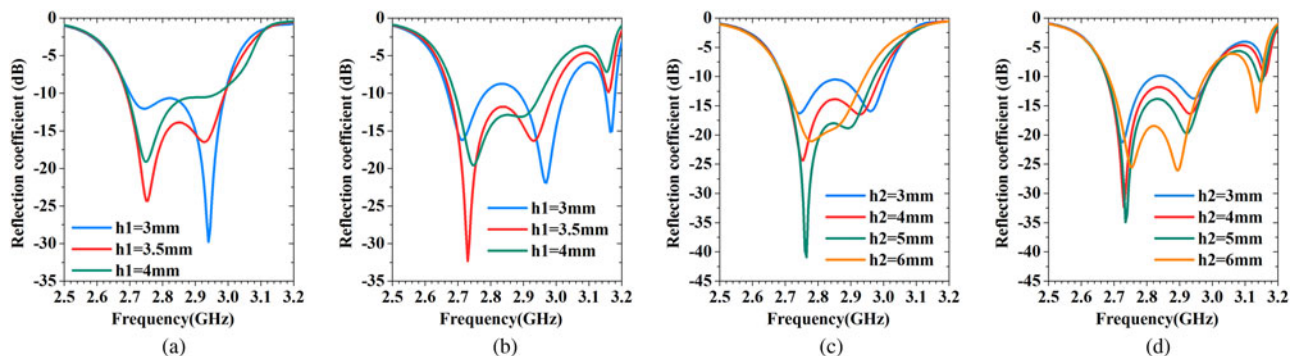| Layer | Material | $\varepsilon_r$ | Thickness (mm) | Upside | Backside |
|-------|----------|-----------------|----------------|--------|----------|
| Sub1 | F4BM350 | 3.5 | 0.8 | Ground and DRAs | Feed network (C band) |
| Sub2 | F4BM265 | 2.65 | 1 | Feedline (S band) | – |
| Sub3 | F4BM265 | 2.65 | 1 | Driven dipole (VP) | Driven dipole (HP) |
| Sub4 | F4BM265 | 2.65 | 1 | Parasitic dipole (VP) | Parasitic dipole (HP) |



**Fig. 2.** Simulated reflection coefficient of S-band dipoles with different values of $h_1$ and $h_2$. (a) Reflection coefficient with different values of $h_1$ for H-port ($h_2 = 4$). (b) Reflection coefficient with different values of $h_1$ for V-port ($h_2 = 4$). (c) Reflection coefficient with different values of $h_2$ for H-port ($h_1 = 3.5$). (d) Reflection coefficient with different values of $h_2$ for V-port ($h_1 = 3.5$).

**Table 3.** Comparison of three feeding schemes

|  | Probe feed | Hybrid feed | Slot coupled |
|--|------------|-------------|--------------|
|  |  |  |  |
| BW (H/V) (MHz) | 500/500 | 770/550 | 740/780 |
| Cross polarization (H/V) (dB) | −20/−20 | −34/−25 | −17/−32 |
| Polarization isolation (dB) | 20 | 48 | 36 |
| Tolerances | Tolerant | Tolerant | Strict |
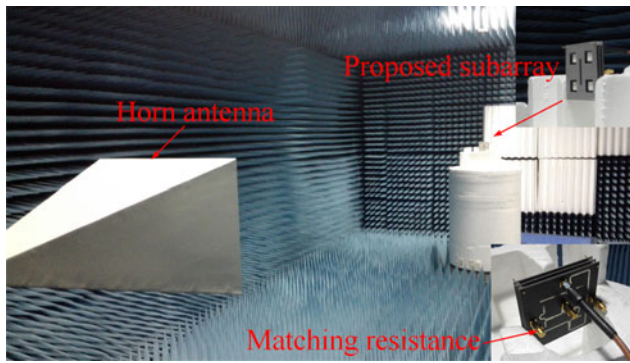
**Fig. 3.** Experimental setup.
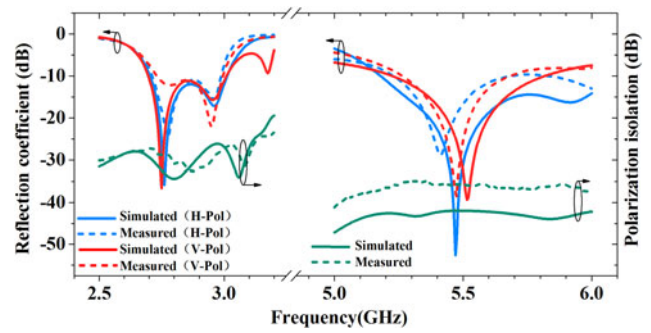


**Fig. 4.** Measured and simulated *S*-parameter of S band port and C band port.



Measured: —— Co-pol ······ Cross-pol
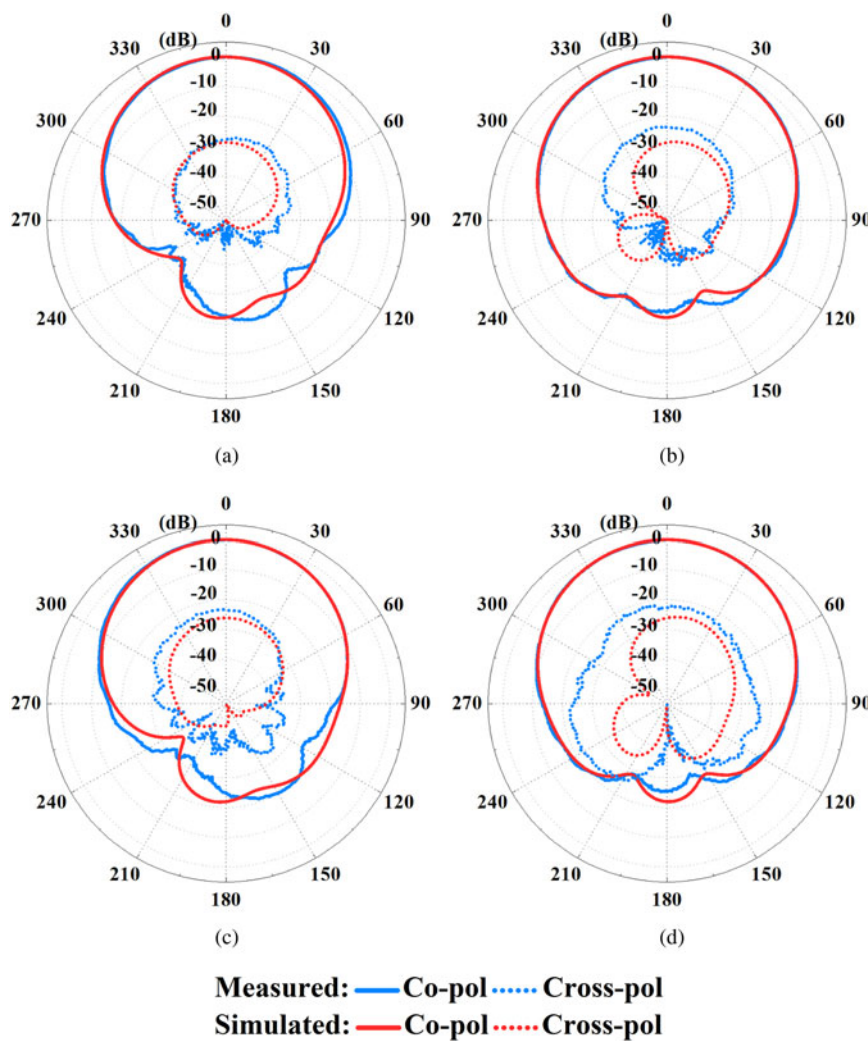Simulated: —— Co-pol ····· Cross-pol

**Fig. 5.** Measured and simulated radiation patterns at S band. (a) H-pol E plane. (b) H-pol H plane. (c) V-pol E plane. (d) V-pol H plane.

and broaden the bandwidth. The feed lines are printed at the upside of sub2, the driven dipoles are printed at sub3, and the parasitic dipoles are printed at sub4. The driven dipoles and parasitic dipoles each excite one resonance point, and we can broaden the bandwidth by connecting the two resonance points, and by introducing two air layers under Sub3 and Sub4, the $Q$ factor of dipoles are decreased, which further broaden the bandwidth. The two sets of stacked microstrip dipoles are crossed in the

center at the positive and negative sides of two substrates respectively for dual-polarized, as Fig. 1 shows.

Several variables can be used to adjust the S band antenna such as the spacing between Sub2 and Sub3 ($h_1$), Sub3 and Sub4 ($h_2$), the spacing between two tuning stubs, the position of tuning stubs, the length of tuning stubs, and the length of dipoles/parasitic dipoles. The $h_1$ and $h_2$ are very crucial variables in that they can affect both polarization ports, but other variables affect only
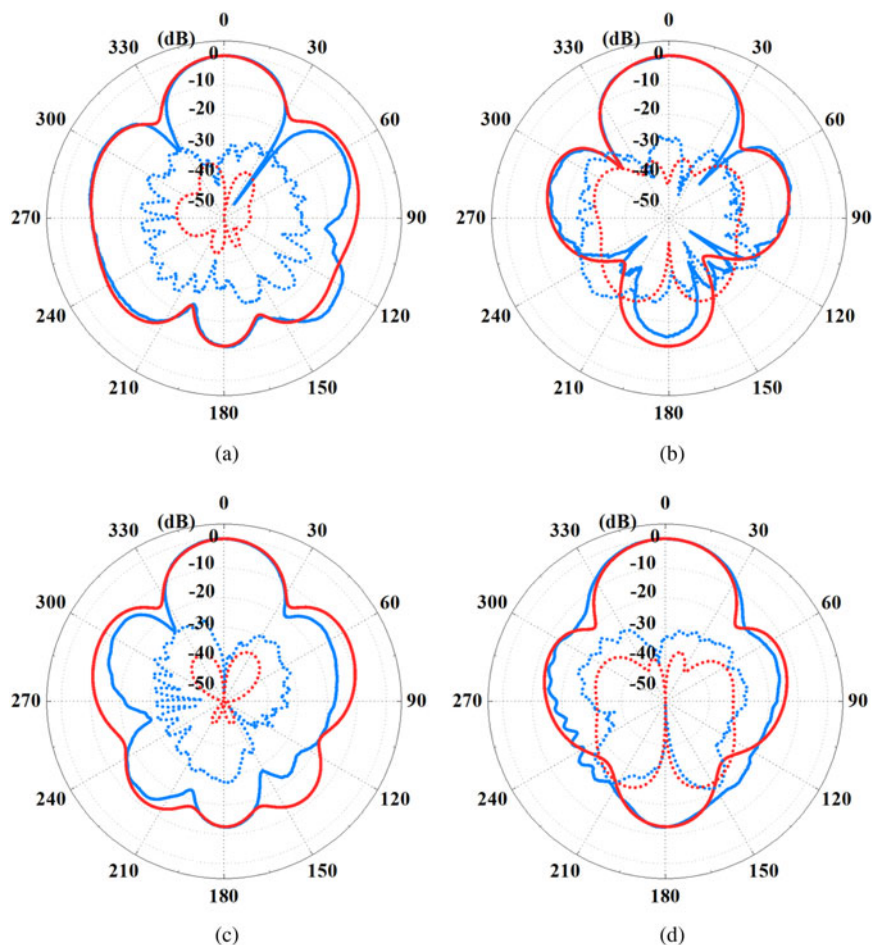
**Fig. 6.** Measured and simulated radiation patterns at C band. (a) H-pol E plane. (b) H-pol H plane. (c) V-pol E plane. (d) V-pol H plane.

one port. Moreover, $h_1$ is more important, because when the spacing between Sub2 and Sub3 changes, the spacing between Sub2 and Sub4 changes too. So adjusting spacing values, especially $h_1$, has the highest priority. Figure 2 shows the simulated reflection coefficient of S-band dipoles with different values of $h_1$ and $h_2$, the change of $h_1$ has a significant influence on the reflection coefficient of both ports, and both ports achieve best reflection coefficient values when $h_1 = 3.5$ mm. Comparatively, the reflection coefficient of two ports is not so sensitive to $h_2$, when $h_2$ is increased from 3 to 6 mm. The worst reflection coefficient value decreased from −10.5 to −18.7 dB for H-port, and from −9.9 to −18.5 dB for V-port, however, when $h_2$ is increased, the two resonance points of both ports would be closer, which leads to a bandwidth loss. Therefore, 4 mm is selected as the value for $h_2$ after trade-off between reflection coefficient and bandwidth. Then we can use the optimized spacing values to adjust other variables for further optimization, and other optimized parameters are shown in Fig. 1(d).

Dual-polarized DRAs ($Al_2O_3$, $\varepsilon_r = 9.8$) working in the fundamental mode are employed as radiating elements for the C band. The resonant frequency of rectangular DRA is determined by its dimensions, materials, and working mode, and can be calculated by the equations given in [25].

In this shared aperture antenna, the feedlines of C band DRAs are reserved under the ground, so three feeding schemes (probe fed,

aperture coupled, and hybrid fed) are selected as candidates. The simulated results are shown in Table 3. Although the bandwidth of hybrid feed DRA is narrower than the slot-coupled DRA, the hybrid feed DRA owns better polarization isolation, lower cross-polarization and has more tolerant of fabrication errors, so that the hybrid feed DRA is selected for radiation element of C band.

DRAs with low dielectric constant material provide desired bandwidth, the "pair-wise" anti-phase feed technique is used to reduce the cross-polarization of array. F4BM265 ($\varepsilon_r = 2.65$) is selected as the substrate of C band in order to make the feed line thinner for setting power dividers of two polarizations. In order to set the $2 \times 2$ DRAs, we need four perforations in Sub2, Sub3, and Sub4 respectively. Feed networks for DRA array are necessary in order to improve integration, and two 4-way 0°/180° differential power dividers for each polarization are designed and printed on the backside of sub1, separated from the feed lines of S band by ground, and in this way, the isolation between bands is improved largely. The structure of C band DRA array is shown in Fig. 1, and some key parameters are given in Fig. 1(e).

## Results and discussion

The proposed antenna is designed and simulated by using Ansoft HFSS15, and the prototype antenna is manufactured and tested to validate the design as shown in Fig. 3. The simulated and
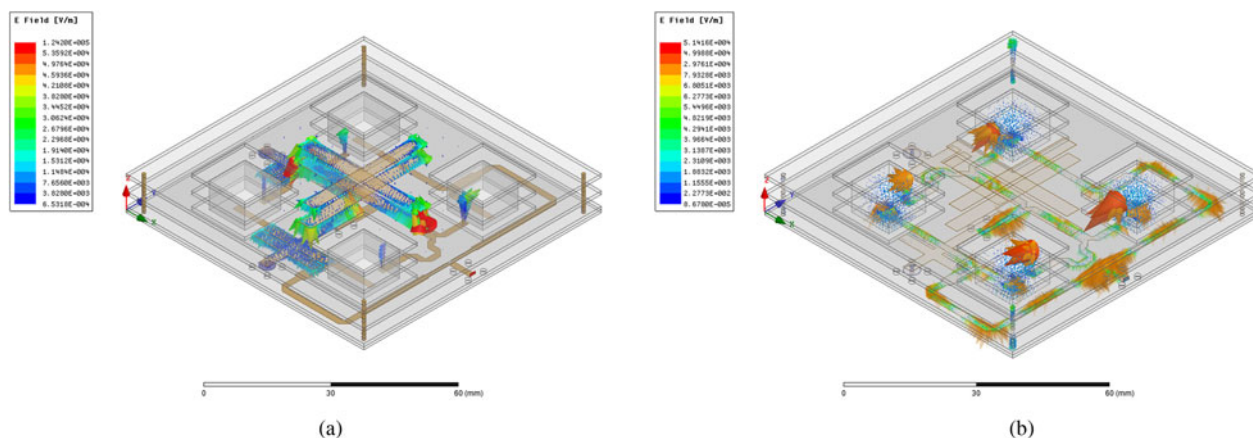
**Fig. 7.** Vector *E* field of proposed antenna. (a) At 2.85 GHz, when only S band is excited. (b) At 5.5 GHZ, when only C band is excited.
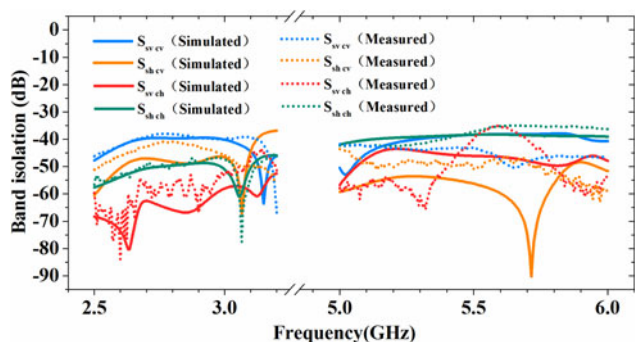


**Fig. 8.** Simulated/measured band isolation.

measured *S*-parameters and radiation patterns for the S band are shown in Figs 4 and 5. A measured bandwidth from 2.72 to 2.99 GHz is achieved for both polarizations, i.e., 9.5%. A good bandwidth of S band is obtained, but a little narrower than simulated, since an uncontrollable spacing would exist between Sub1 and Sub2 due to the solder joint, besides, the length of the hard plastic tube may also produce a little deviation. The isolation is over 25 dB between the two orthogonal ports in the operating band, the co-polarization radiation pattern is symmetrical, and cross-polarization levels are better than −20 dB in both planes, which shows good agreement between simulated and measured results.

The simulated and measured *S*-parameters for the C band are shown in Fig. 4. The antenna has an impedance bandwidth from

5.25 to 5.7 GHz for both orthogonal ports. The obtained bandwidth is 450 MHz, and there is a 50 MHz frequency shift in the resonance points between simulated and measured results since the dielectric constant and the size of DRAs is not precise enough. The measured isolation between polarizations is better than 35 dB, 5 dB lower than simulated data, and this may be caused by the influence of manufacturing and assembly error. The radiation patterns of C band are shown in Fig. 6, the co-polarization radiation pattern of the C band is symmetrical and accord with simulated. However, the cross-polarization level within the main lobe is less than −25 dB, which is worse than simulated, because the position errors of the DRA array would occur inevitably and the symmetrical characteristic of the array is affected when fixing DRAs on the ground by glue manually.

Since elements of two bands are set in the same aperture, so the mutual coupling is worthy of being studied, the simulated distribution of the vector *E* field is shown in Fig. 7. At 2.85 GHz, when only S band is excited, there is a strong *E* field distribution on S band feed lines, driven dipoles, and parasitic dipoles, and a weaker *E* field distribution on C band feeding probe, however, there is no *E* field distribution in DRAs because the frequency is far lower than the frequency of fundamental mode and the DRAs would not be excited, and benefited from the non-metal structure of DRAs, the parasitic capacitance between DRAs and dipoles would not be produced and *E* filed would hardly be coupled into DRAs. Furthermore, there is almost no *E* field distribution on the feed network of C band benefited from the separation by ground. At 5.5 GHz, when only C band is excited, the strong *E* field is distributed in DRAs and feed networks of C

**Table 4.** Comparison between the proposed antenna and previous models

| | Band | Polar | BW (%) | Cross-polarization (dB) | Polarization isolation (dB) | Band isolation (dB) |
|---|---|---|---|---|---|---|
| [3] | C/X | DLP/DLP | 4.8/6.1 | −24/−26 | 25/23 | – |
| [11] | S/X | DLP/DLP | 8.9/17 | −26/−31 | 20/20 | – |
| [13] | S/X | DLP/DLP | 10.7/6 | −/30 | 32/25 | – |
| [14] | S/X | DLP/DLP | 1.03/1.8 | −10/−16 | 30/24 | 25.3 |
| [19] | L/S | LP/LP | 54/25 | −15/−20 | – | 25 |
| [22] | S/X | RHCP/LP | 19.3/22 | −17/−15 | – | 32 |
| This paper | S/C | DLP/DLP | 9.5/8.2 | −20/−25 | 25/35 | 35 |

band. In contrast, there is almost no *E* field distribution on antennas and feed lines of S band. When a single band is excited, the weaker *E* field distributes on the antenna of another band, the better isolation shared aperture antenna has, which indicate the good isolation between two bands. Besides, the simulated and measured isolation results are also shown in Fig. 8, and we can see the worst-case measured isolation between bands is 35 dB, which reveals that good isolation and little mutual interference are obtained.

Some main performances of several small FR shared-aperture antennas are compared in Table 4. The comparison results show that the proposed antenna has good comprehensive performance and the main advantage of the proposed shared-aperture antenna is high isolation.

## Conclusions

In this paper, a novel DBDP shared-aperture antenna with a FR of about 1:2 is presented. Several techniques are used to broaden the bandwidth, improve the polarization isolation, and reduce the cross-polarization level. Furthermore, high isolation between bands and low mutual interference are achieved benefited from the use of DRA. The prototype antenna is fabricated and measured. The measured results show that the antenna covers the frequency bands of 2.72–2.99 GHz and 5.25–5.7 GHz with $S_{11}$ below −10 dB, the isolation between polarizations is better than 25 dB for S band and 35 dB for C band, the cross-polarization level for S and C bands is lower than −20 and −25 dB in the main lobe respectively, and the isolation between the two ports is over 35 dB. The proposed antenna has many advantages such as low cost, high integration, and low mutual interference. In addition, the proposed antenna has geometrical symmetry, which shows it has the potential of expanding into a large aperture.

## References

1. **Zhang J-D, Wu W and Fang D-G** (2016) Dual-band and dual-circularly polarized shared-aperture array antennas with single-layer substrate. *IEEE Transactions on Antennas and Propagation* **64**, 109–116.
2. **Li M, Wu Y, Qu M, Jiao L and Liu Y** (2018) Triband planar shared-aperture antenna array with similar shaped radiation patterns. *Microwave and Optical Technology Letters* **60**, 2284–2288.
3. **Mao C-X, Gao S, Wang Y, Luo Q and Chu Q-X** (2017) A shared-aperture dual-band dual-polarized filtering-antenna-array with improved frequency response. *IEEE Transactions on Antennas and Propagation* **65**, 1836–1844.
4. **Shafai LL, Chamma WA, Barakat M, Strickland PC and Seguin G** (2000) Dual-band dual-polarized perforated microstrip antennas for SAR applications. *IEEE Transactions on Antennas and Propagation* **48**, 58–66.
5. **Shen F, Yin C, Guo K, Wang S, Gong Y and Guo Z** (2019) Low-cost dual-band multi-polarization aperture-shared antenna with single-layer substrate. *IEEE Antennas and Wireless Propagation Letters* **18**, 1337–1341.
6. **Meng CX, Shen HW, Sun Z, Zhong SS and Esselle KP** (2011) A novel L/C-band dual-polarized half-perforated antenna element for SAR arrays, *Asia-Pacific Microwave Conference, Melbourne, VIC*.
7. **Vetharatnam G, Boon Kuan C and Hean Teik C** (2005) Combined feed network for a shared-aperture dual-band dual-polarized array. *IEEE Antennas and Wireless Propagation Letters* **4**, 297–299.
8. **Zhou S-G, Yang J-J and Chio T-H** (2015) Design of L/X-band shared aperture antenna array for SAR application. *Microwave & Optical Technology Letters* **57**, 2197–2204.
9. **Pozar DM and Targonski SD** (2001) A shared-aperture dual-band dual-polarized microstrip array. *IEEE Transactions on Antennas and Propagation* **49**, 150–157.
10. **Zhuo S-G and Chio T-H** (2011) A shared-aperture dual-wideband dual-polarized stacked microstrip array. *Microwave & Optical Technology Letters* **54**, 486–491.
11. **Qu X, Zhong SS, Zhang YM and Wang W** (2007) Design of an S/X dual-band dual-polarised microstrip antenna array for SAR applications. *IET Microwaves Antennas and Propagation* **1**, 513–517.
12. **Kong L-B, Zhong S-S and Sun Z** (2012) Broadband microstrip element design of a DBDP shared-aperture SAR array. *Microwave & Optical Technology Letters* **54**, 133–136.
13. **Sun Z, Zhong SS, Kon LB, Gao C, Wan W and Jin MP** (2012) Dual-band dual-polarised microstrip array with fractional frequency ratio. *Electronics letters* **48**, 674–676.
14. **Hsu S-H, Ren Y-J and Chang K** (2009) A dual-polarized planar-array antenna for S-band and X-band airborne applications. *IEEE Antennas and Propagation Magazine* **51**, 70–78.
15. **Yi L, Ya H, Dai M, Wang H and Yang H** (2014) Design of a Ka/Ku Dual-Band Dual-Polarized Array. *Proceedings of 2014 3rd Asia-Pacific Conference on Antennas and Propagation, Harbin*.
16. **Mao C-X, Gao S, Wang Y, Chu Q-X and Yang X-X** (2017) Dual-band circularly polarized shared-aperture array for C-/X-band satellite communications. *IEEE Transactions on Antennas and Propagation* **65**, 5171–5178.
17. **Kong L and Xu X** (2018) A compact dual-band dual-polarized microstrip antenna array for MIMO-SAR applications. *IEEE Transactions on Antennas and Propagation* **66**, 2374–2381.
18. **Zhang X-Y, Xue D, Ye L-H, Pan Y-M and Zhang Y** (2017) Compact dual-band dual-polarized interleaved two-beam array with stable radiation pattern based on filtering elements. *IEEE Transactions on Antennas and Propagation* **65**, 4566–4575.
19. **Naik H, Awasthi AK and Harish AR** (2019) Shared-aperture dual-band orthogonally polarised antenna array for L-band and S-band applications. *IET Microwaves, Antennas & Propagation* **13**, 431–435.
20. **Naishadham K, Li R, Yang L, Wu T, Hunsicker W and Tentzeris M** (2013) A shared-aperture dual-band planar array with self-similar printed folded dipoles printed folded dipoles. *IEEE Transactions on Antennas and Propagation* **61**, 606–613.
21. **Zhou S-G, Tan P-K and Chio T-H** (2013) Wideband, low profile P- and Ku-band shared aperture antenna with high isolation and low cross-polarisation. *IET Microwaves, Antennas & Propagation* **7**, 223–229.
22. **Wang K, Liang X, Zhu W, Geng J, Li J, Ding Z and Jin R** (2018) A dual-wideband dual-polarized aperture-shared patch antenna with high isolation. *IEEE Antennas and Wireless Propagation Letters* **17**, 735–738.
23. **Gulam Nabi Alsath M, Kanagasabai M and Arunkumar S** (2012) Dual-band dielectric resonator reflectarray for C/X-bands. *IEEE Antennas and Wireless Propagation Letters* **11**, 1253–1256.
24. **Levine E, Malamud G, Shtrikman S and Treves D** (1989) A study of microstrip array antennas with the feed network. *IEEE Transactions on Antennas and Propagation* **37**, 426–434.
25. **Mongia LRK and Ittipiboon A** (1997) Theoretical and experimental investigations on rectangular dielectric resonator antennas. *IEEE Transactions on Antennas and Propagation* **45**, 1348–1356.

**JiaChen Xu** was born in Shannxi Province, China, in 1991. He received his B.Sc. degree and M.Sc. degree from the School of Electrical and Information, Northwestern Polytechnical University in Xi'an city, China, in 2013 and 2016, respectively. He is presently working on his doctoral degree at the School of Electronics and Information, Northwestern Polytechnical University in Xi'an city, China. His research interests include dielectric resonator antennas and shared aperture arrays.
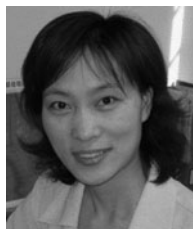
**BoZhang Lan** was born in Shannxi Province, China, in 1992. He received his B.S. degree in electronic science and technology from the HeFei University of Technology in HeFei city, China in 2014, and received his M.S. degree in electromagnetic filed and microwave technology from Northwestern Polytechnical University in Xi'an city, China in 2016. He is working toward his Ph.D. degree at Northwestern Polytechnical University. His research interests include reconfigurable antennas and microwave filters.

**ChenJiang Guo** was born in Shannxi Province, China, in 1963. He is CIE Senior Member, Antenna Society Committee Member. He received his M.Sc., B.Sc., and Ph.D. from the School of Electronics and Information, Northwestern Polytechnical University in Xi'an city, China, in 1984, 1987, and 2007, respectively. He is a professor in the School of Electronics and Information, NWPU. He has published more than 140 research papers. His research interests include EMI/EMC, antenna theory and design, and microwave circuit design.

**JiaKai Zhang** was born in Shannxi Province, China, in 1990. He received his M.Sc. and B.Sc. degrees from the School of Electronics and Information, Northwestern Polytechnical University in Xi'an city, China, in 2012 and 2015, respectively. He is presently working on his doctoral degree at the School of Electronics and Information, Northwestern Polytechnical University in Xi'an city, China. His research interests include electromagnetic metamaterials and antenna RCS reduction.

**Jun Ding** was born in Shannxi Province, China, in 1964. She received her M.Sc., B.Sc., and Ph.D. from the School of Electronics and Information, Northwestern Polytechnical University in Xi'an city, China, in 1986, 1989, and 2005, respectively. She is a professor at the School of Electronics and Information, NWPU. She has published more than 100 research papers. Her research interests include electromagnetic metamaterials, antenna theory and design, and microwave circuit design.